Published in final edited form as:
Free Radic Biol Med. 2009 February 1; 46(3): 406–413. doi:10.1016/j.freeradbiomed.2008.10.037.

Inhibition of mitochondrial permeability transition by cyclosporin A prevents pyrazole plus lipopolysaccharide-induced liver injury in mice

Jian Zhuge and **Arthur I. Cederbaum**
Department of Pharmacology and Systems Therapeutics, Mount Sinai School of Medicine, New York, NY 10029, USA

Abstract

Previous results showed that pyrazole potentiates lipopolysaccharide (LPS)-induced liver injury in mice. Mechanisms involved overexpression of cytochrome P450 2E1 (CYP2E1), oxidative stress, activation of c-Jun N-terminal kinase (JNK) and p38 mitogen-activated protein kinase (MAPK). The current study was carried out to test the hypothesis that the mitochondria permeability transition (MPT) plays a role in this pyrazole plus LPS toxicity. Mice were injected intraperitoneally with pyrazole for two days, followed by a challenge with LPS with or without treatment with cyclosporin A (CsA), an inhibitor of the MPT. Serum alanine aminotransferase and aspartate aminotransferase were increased by pyrazole plus LPS treatment, and CsA treatment could attenuate these increases. CsA also prevented pyrazole plus LPS-induced hepatocyte necrosis. Formation of 4-hydroxynonenal (HNE) protein adducts and 3-nitrotyrosine (3-NT) protein adducts in liver tissue were increased by the pyrazole plus LPS treatment, and CsA treatment blunted these increases. Swelling, cytochrome c release from mitochondria to the cytosol, and lipid peroxidation were increased in mitochondria isolated from the pyrazole plus LPS-treated mice, and CsA treatment prevented these changes. CsA did not prevent the increased levels of inducible nitric oxide synthase (iNOS), tumor necrosis factor-α (TNF-α), pp38 MAPK and p-JNK2 levels. In conclusion, while CsA does not prevent elevations in upstream mediators of the pyrazole plus LPS toxicity (iNOS, TNF-α, CYP2E1, MAPK), CsA protects mice from the pyrazole plus LPS-induced liver toxicity, by preventing MPT, release of cytochrome c and decreasing mitochondrial oxidative stress. These results indicate that mitochondria are the critical target of pyrazole plus LPS in mediating liver injury.

Keywords

Mitochondrial permeability transition; Necrosis; Cyclosporin A; Pyrazole; Lipopolysaccharide; Reactive oxygen species

Correspondence to: Arthur I. Cederbaum Ph. D., Department of Pharmacology and Systems Therapeutics, Box 1603, Mount Sinai School of Medicine, One Gustave L. Levy Place, New York, NY 10029, USA. E-mail: Arthur.cederbaum@mssm.edu. Phone: +1-212-241-7285. Fax: +1-212-996-7214.

Introduction

Endotoxemia and endotoxin-mediated hepatocellular damage play a crucial role in the pathogenesis of alcoholic liver disease. Elevated intestinal permeability appears to be the major factor involved in the mechanism of alcoholic endotoxemia and the pathogenesis of alcoholic liver disease [1]. Induction of cytochrome P450 2E1 (CYP2E1) by ethanol is one pathway by which ethanol can induce oxidative stress. CYP2E1 metabolizes and activates many toxicological substrates, including ethanol, to more reactive, toxic products. CYP2E1 is an effective generator of reactive oxygen species (ROS) such as the superoxide anion radical and hydrogen peroxide and, in the presence of iron catalysts, produces powerful oxidants such as the hydroxyl radical [2,3].

Lipopolysaccharide (LPS) and CYP2E1 are considered two independent risk factors in alcohol liver injury. In order to study their possible mutual interactions in vivo, rodent models were established by using pyrazole to induce CYP2E1 then followed by LPS injection [4-6]. Liver injury was observed after this combined pyrazole plus LPS treatment under conditions in which pyrazole alone or LPS alone do not cause liver injury. The mechanism of the liver injury included induction of CYP2E1, oxidative stress [5] activation of c-Jun N-terminal kinase (JNK) and p38 mitogen-activated protein kinase MAPK) and mitochondrial injury [6]. While treatment of mice with pyrazole is known to alter expression of many genes [7], the pyrazole potentiation of LPS/tumor necrosis factor (TNF)-α liver injury was mediated, at least in part, by CYP2E1, since injury was prevented by chlormethiazole, a CYP2E1 inhibitor, and in CYP2E1 knockout mice [4-6]. Mitochondria isolated from the pyrazole plus LPS-treated mice underwent calcium-induced swelling to a greater extent than did mitochondria from control or pyrazole alone or LPS alone-treated mice [6], suggesting the occurrence of a mitochondrial permeability transition (MPT), especially since addition of cyclosporin A (CsA) in vitro blocked the elevated swelling [6]. However, it is still not known whether this MPT plays a role in the pyrazole plus LPS liver toxicity in vivo.

The MPT is a sudden nonselective increase of mitochondrial membrane permeability of the inner mitochondrial membrane to solutes of molecular mass less than 1500 Da. The MPT leads to loss of mitochondrial membrane potential, mitochondrial swelling, and rupture of the outer mitochondrial membrane [8,9]. Cyclophilin D plays a critical role in regulation of the MPT pore in cell death as confirmed by cyclophilin D knockout mice studies; the adenine nucleotide translocase may serve some regulatory function [8]. CsA, a specific inhibitor of the MPT [10], has been used to protect mice from acetaminophen-, Fas-, and 1,1-dichloroethylene-induced liver injury [11-13].

In this study, CsA was applied to the pyrazole plus LPS mouse model, to evaluate whether it can protect against liver injury and thus provide some evidence that the MPT plays a role in pyrazole plus LPS-induced liver injury.

Materials and Methods

Mice treatment

All mice received humane care in compliance with the “Guide for the Care and Use of Laboratory Animals” prepared by the Association for Assessment and Accreditation of Laboratory Animal Care (March 1999), and approval was obtained from The Mount Sinai Animal Care and Use Committee. Male C57BL/6 mice (Charles River Laboratories, Wilmington, MA), 8 weeks old were injected intraperitoneally with pyrazole (Aldrich Chemistry), an inducer of CYP2E1, 150 mg/kg body weight, once a day for 2 days, and after an overnight fast, one dose of LPS (4 mg/kg) (From Escherichia coli 055:B5, catalog #L2880, lot #114k4103, Sigma Chemical Co., St. Louis, MO) was injected intraperitoneally. Some of

these mice were also injected intraperitoneally with CsA (Alexis Biochemicals, Lausen, Switzerland), dissolved in corn oil, 100 mg/kg body weight once with the LPS (Pyrazole+LPS +CsA group) or with the same volume of corn oil (Pyrazole+LPS group). Control mice were injected intraperitoneally with normal saline and corn oil. Some mice were injected intraperitoneally with pyrazole and corn oil or LPS and corn oil (Pyrazole and LPS groups). Mice were killed 24 h after the last injection, serum was collected and liver tissues were split into several pieces. Some pieces were snap frozen and stored at -70°C, while other pieces were fixed with formalin for histology and immunohistochemistry. Serum alanine aminotransferase (ALT) and aspartate aminotransferase (AST) levels were assayed with the Infinity ALT and AST liquid stable reagent (Thermo Electron Corp. Pittsburgh, PA).

Liver histology and immunohistochemistry

Sections from formalin fixed liver tissues were processed, embedded, sectioned and stained with hematoxylin and eosin by the Biorepository Cooperative and Histology Service Shared Research Facility at Mount Sinai School of Medicine. Immunohistochemical staining of 4-hydroxynonenal (HNE) protein adducts and 3-nitrotyrosine (3-NT) protein adducts in liver tissue was performed using rabbit anti-HNE (1:50, Calbiochem, San Diego, CA) and rabbit anti-3-NT (1:100, Upstate, Lake Placid, NY) antibodies, respectively and an immunoperoxide secondary detection system (Chemicon, Temecula, CA).

Mitochondrial swelling

Mitochondria were isolated from fresh liver tissue by differential centrifugation and calcium-induced mitochondrial swelling was assayed using 5 mM glutamate plus 2.5 mM malate as substrates according to a previously described method [6].

Glutathione (GSH), S-Adenosyl-L-Methionine (SAM) and lipid peroxidation measurement

GSH levels in liver homogenate and mitochondria were determined using the fluorometric substrate o-phthalaldehyde (MP Biomedicals, LLC, Aurora, Ohio) [14]. Liver SAM levels were assayed by high performance liquid chromatography as previously described [15]. Malondialdehyde (MDA) levels in mitochondria was assayed as thiobarbituric acid reactive substrates as described previously [16].

Western blot analysis

Liver homogenate, 100 μg protein, was used for Western blot analysis of TNF-α (Rabbit anti-mouse TNF-α, 1 μg/ml, Fitzgerald Industries International Inc., Concord, MA), inducible nitric oxide synthase (iNOS) (Rabbit anti-iNOS, 1: 5000, Millipore Corp., Billerica, MA), phosphorylated and total p38 and JNK (Rabbit anti-pp38, p38, JNK1, and mouse anti-p-JNK antibodies, 1: 1000, Santa Cruz Biotechnology, Inc.). Mitochondrial lysate, 100 μg protein, was used for Western blot analysis of cytochrome c (Mouse anti-cytochrome c, clone 7H8.2C12, 1:1000, BD Biosciences, San Jose, CA), BAX (Ab-1, rabbit, 1:1000, Calbiochem), BCL-2, BID, BCL-xS/L (Rabbit, 1: 1000, Santa Cruz Biotechnology, Inc., Santa Cruz, CA). The 7700 × g cytosol fraction, 100 μg protein, was used for Western blot analysis of cytochrome c (1:1000, BD Biosciences). After washing, the membranes were incubated for 1 h with anti-mouse, rabbit, or goat IRDye secondary antibodies (1:10000, LI-COR Bioscience Inc., Lincoln, NE) respectively, washed, and scanned with the Odyssey infrared imaging system (model 9120, LI-COR Bioscience Inc.). Membranes were also incubated with monoclonal anti-β-actin antibody (1: 10000, Santa Cruz Biotechnology Inc.) as a loading control or goat anti-manganese superoxide dismutase (SOD2) antibody (G20, 1: 1000, Santa Cruz Biotechnology Inc.) as a mitochondrial loading control. Some of the membranes were incubated with relevant horseradish peroxidase conjugated secondary antibodies (1:10000). Detection by the chemiluminescence reaction was carried out for 1 min using the ECL Western blotting substrate

(Pierce Biotechnology, Rockford, IL), followed by exposure to CL-XPosure film (Pierce Biotechnology). Bands were quantified by the ImageJ image processing program developed by Wayne Rasband (National Institute of Mental Health, Bethesda, Maryland, USA). As mentioned in the BD Pharmingen technical data sheet, cytochrome c in the cytoplasm "might exist in polymeric forms, appearing as a 58-60 kD band by Western blot analysis, rather than the monomeric form. Monomeric cytochrome c migrates at a reduced molecular weight of 15 kD". For example, tocotrienols induced a massive release of cytochrome c from rat pancreatic stellate cells which was detected as a 58 kD polymeric form in the cytosol [17].

Statistical analysis

Data are shown in the figures are presented as means ± SD of 3 to 5 mice per group. Experiments were repeated 2-3 times with another 3-5 mice per group with similar results (total 6-15 mice in each group). Statistical differences for the data shown in the figures were analyzed by one-way or two-way ANOVA followed by multiple comparisons performed with post hoc Bonferroni test (SPSS version 10.0) with $P<0.05$ as the level of significance.

Results

CsA protects mice from pyrazole plus LPS-induced liver injury

We have previously shown that treatment of mice with pyrazole plus LPS or pyrazole plus TNF-α leads to enhanced calcium-induced mitochondrial swelling compared to mice treated with saline or pyrazole alone or LPS/ TNF-α alone [6]. Addition of 2 μM CsA in vitro blunted the swelling in all groups of mitochondria and prevented the elevated swelling in the mitochondria from pyrazole plus LPS or pyrazole plus TNF-α groups [6]. We have also shown that addition of 2 μM CsA in vitro prevented the release of cytochrome c from mitochondria from wild type and SOD1 knockout mice fed ethanol chronically [18]. The goal of the current study was to evaluate the effectiveness of in vivo administration of CsA in protecting against pyrazole plus LPS toxicity. Serum ALT and AST levels, which are indices of liver necrosis, were increased 7- and 3-fold respectively after pyrazole plus LPS treatment as has been described previously [4-6]. CsA treatment attenuated the increase produced by the pyrazole plus LPS treatment (Fig. 1A). Hematoxylin and eosin staining of liver tissue showed pyrazole plus LPS induced extensive liver zonal necrosis and CsA treatment prevented the liver necrosis (Fig.1B).

Pyrazole plus LPS-induced oxidative/nitrosative stress

HNE is derived from the oxidation of membrane n-6-polyunsaturated fatty acids, especially arachidonic acid and linoleic acid, the two most represented polyunsaturated fatty acids in biomembranes [19]. HNE-protein adducts are considered a marker of lipid oxidation during liver injury [19]. 3-NT-protein adducts are one marker of peroxynitrite production in vivo [20]. Nitration, a biological process derived from the biochemical interaction of NO or NO-derived secondary products with ROS such as superoxide radical, nitrites free and protein-associated tyrosine residues to produce 3-NT adducts [21]. Immunohistochemistry detection for HNE and 3-NT protein adducts showed staining for these adducts was increased in the pyrazole plus LPS-treated mice (Fig. 2A). CsA treatment largely prevented the increase in HNE and 3-NT adducts.

Intracellular GSH levels were increased 43% in livers of pyrazole-treated mice compared to control mice (Fig. 2B), as previously found in pyrazole-treated Sprague-Dawley rats [22] or pyrazole-treated obese mice [23]. This may reflect a metabolic adaptation to the oxidative stress induced by CYP2E1. Pyrazole plus LPS treatment reduced the GSH to 34% of normal levels. CsA treatment slightly but not significantly attenuated this reduction of GSH levels (Fig. 2B).

SAM has been shown have hepatoprotective effects. Neither pyrazole nor pyrazole plus LPS, with and without CsA treatment, had any effect on SAM levels in the liver (Fig. 2C).

Levels of TNF-α, iNOS and activation of p38 MAPK and JNK

Previous experiments showed that the pyrazole plus LPS treatment elevated levels of TNF-α, iNOS and activated p38 MAPK and JNK, but not ERK [6]. These increases were important in the pyrazole plus LPS-induced liver injury since the injury could be lowered by inhibitors of p38 MAPK and JNK [6], or by an inhibitor of iNOS (Wu et al, manuscript submitted), and mimicked by TNF-α replacing LPS [6]. Could the protection by CsA reflect blunting of the production of TNF-α or elevation of iNOS, p38 MAPK, or JNK? TNF-α levels in liver homogenates were elevated by the pyrazole plus LPS treatment, however, CsA treatment did not alter this increase in TNF-α (Fig. 3A). Similarly, iNOS levels were elevated by the pyrazole plus LPS treatment, however, CsA treatment did not attenuate this induction (Fig. 3B). p38 and JNK2 activation (phosphorylation) were increased in pyrazole plus LPS-treated mice compared to control mice (Fig. 3C, D) as previously reported [6]. CsA treatment did not attenuate the increase in MAPK (Fig. 3C, D). Phosphorylation of JNK1 was not observed under these conditions. Interestingly, in experiments carried out in JNK1 or JNK2 knockout mice, JNK2 but not JNK1 was found to be critical for activation of the TNF-α mitochondrial death pathway [24]. Further experiments will be necessary to evaluate the role of JNK1 versus JNK2 in the pyrazole plus LPS liver injury.

These experiments show that CsA did not prevent against the pyrazole plus LPS-induced liver injury by blunting the production of TNF-α, the elevation of iNOS, or the activation of p38 MAPK or JNK [2]. The CsA treatment also had no effect on levels or activity of CYP2E1 (Data not shown).

Mitochondrial swelling and cytochrome c release from mitochondria

Mitochondrial swelling was assessed to reflect MPT induction in isolated mitochondria [25]. A large amplitude swelling was shown to occur in mitochondria isolated from pyrazole plus LPS-treated mice as compared to mitochondria from control mice (Fig. 4A, two-way ANOVA, $P<0.001$). CsA treatment prevented the pyrazole plus LPS-induced mitochondrial swelling (Fig. 4A, two-way ANOVA, $P<0.001$), restoring swelling to the control rates.

Western blot analysis showed that while a significant decline of cytochome c in mitochondria could not be detected, an over 2 fold increase in cytochrome c levels in the postmitochondrial cytosol fraction occurred after the pyrazole plus LPS treatment (Fig. 4B). CsA treatment completely blocked this release of cytochrome c from mitochondria (Fig. 4B).

Levels of BCL-2 family proteins

Pro-apoptotic and anti-apoptotic members of the BCL-2 family proteins play critical roles in regulating the MPT and cytochrome c release [26]. Mitochondrial levels of BCL-2 and BCL-xL, two major anti-apoptotic proteins, and BAX, BID, and BCL-xS, major pro-apoptotic proteins were evaluated. Treatment with pyrazole plus LPS increased BCL-2 levels 50%, but did not alter BCL-xL levels (Fig. 5A, D) compared to control mitochondria. The pyrazole plus LPS treatment increased the levels of BAX, BID, and BCL-xS, 2-2.5 fold (Fig. 5B, C, D). We speculate that the larger increase in these pro-apoptotic family proteins overcomes the smaller increase in anti-apoptotic BCL-2 to promote the pyrazole plus LPS-induced MPT. CsA treatment had no effect on these pyrazole plus LPS-induced changes in BCL-2 family proteins (Fig. 5)

Mitochondrial MDA and GSH levels

Mitochondrial MDA levels were increased 45% after pyrazole plus LPS treatment as compared to control mitochondria (Fig. 6A). CsA treatment completely prevented this elevation of mitochondrial lipid peroxidation. LPS alone lowered mitochondrial GSH compared to pyrazole alone treatment. Mitochondrial GSH levels were increased after the pyrazole plus LPS plus CsA treatment compared to that of pyrazole plus LPS treatment, similar to values found for the pyrazole alone-treated mice (Fig. 6B). Thus, the CsA treatment lowered mitochondrial lipid peroxidation in association with an increase in mitochondrial GSH levels.

Discussion

Chronic ethanol consumption induces oxidative stress and elevates LPS/TNF-α levels in the liver, both of which play key roles in liver injury [27-30]. Ethanol treatment elevates CYP2E1 levels and this increase in CYP2E1 may contribute to pathways by which ethanol induces oxidative stress [31-33]. Increased CYP2E1 expression sensitized hepatocytes to TNF-α toxicity as mediated via a c-Jun cell death pathway [34]. We have shown that increasing CYP2E1 levels via treatment with pyrazole sensitize rats and mice to LPS or TNF-α–induced hepatotoxicity, and that toxicity was associated with elevated oxidative stress, activation of p38 MAPK and JNK, and mitochondrial injury [4-6]. The latter included increases in calcium-induced mitochondrial swelling, elevated MDA levels, lower GSH levels [6]. It is not clear if the mitochondrial injury and/or MPT are important for the pyrazole plus LPS-induced liver injury or are consequences of the liver injury, i.e. are not central to the overall mechanism of liver injury in this model. The goal of this report was to evaluate whether CsA, a classic inhibitor of the MPT, would blunt the pyrazole plus LPS-induced mitochondrial damage, and if so, would prevent the liver injury.

Injecting pyrazole plus LPS-treated mice with CsA resulted in a decrease in mitochondrial swelling as compared to pyrazole plus LPS corn oil controls thus establishing that CsA lowers/prevents the MPT under these conditions. The CsA treatment prevented release of cytochrome c into the cytosolic fraction and also decreased mitochondrial MDA levels while elevating mitochondrial GSH levels. Thus, treatment with CsA protects against the pyrazole plus LPS-induced mitochondrial injury. Associated with this protection against mitochondrial injury is a protection against the pyrazole plus LPS-induced liver injury and formation of HNE and 3-NT protein adducts. This would suggest that damage to the mitochondria plays a central role in the pyrazole plus LPS liver injury and oxidative/nitrosative stress. The CsA treatment did not prevent induction of previously identified upstream factors from the mitochondria which mediate pyrazole plus LPS liver injury such as CYP2E1, TNF-α, iNOS and p38 MAPK and JNK [4-6], further suggesting that the site of action for CsA protection is the mitochondria. These results indicate that mitochondria are the critical target of pyrazole plus LPS in mediating liver injury.

Since induction of CYP2E1, TNF-α, and iNOS increases ROS/reactive nitrogen species, it is not clear why CsA decreases HNE and 3-NT adducts in the liver after pyrazole plus LPS treatment when the CsA treatment is not blunting the increases in these agents. This would suggest that the mitochondria, besides being a target for ROS, are also important in generating additional ROS under these conditions i.e. the MPT is elevating ROS production, and CsA, by preventing the MPT, lowers ROS production. It has been proposed that MPT is a significant cause of ROS generation [35] e.g. in calcium uptake studies by mitochondria, twenty one CsA analogs lowered mitochondrial ROS production with an efficacy which paralleled their potency of inhibiting the MPT [36]. “ROS-induced ROS release (RIRR)” is generated by circuits requiring mitochondrial membrane channels including the MPT pore and the inner membrane anion channel (IMAC) [37-39]. The accumulated exposure to ROS leads to an oxidant stress burden in mitochondria that can reach a threshold (MPT ROS threshold) level capable of

inducing the MPT pore and can trigger the opening of one of the requisite mitochondrial channels (MPT pore or IMAC), which in turn leads to the simultaneous collapse of mitochondrial membrane potential and a transient increase in ROS generation by the electron transfer chain [37,40]. Release of this ROS burst to the cytosol could potentially function as a "second messenger" to active RIRR in neighboring mitochondria. Thus mitochondria-to-mitochondria RIRR may constitute a positive feedback mechanism for enhanced ROS production leading to potentially significant mitochondrial and cellular injury [37].

The release of cytochrome c from the mitochondria may also enhance mitochondrial ROS production as a result of a lower efficiency of electron transfer. The mechanisms of cytochrome c release remain controversial [41]. One proposal is that pro-apoptotic BCL-2 family members, such as tBID, BAX and BAK, promote formation of specific cytochrome c release channels in the mitochondrial outer membrane [41,42]. Another mechanism proposes that pores form in the inner membrane that nonspecifically conducts solutes up to 1500 Da. Opening of these pores, the MPT pore, leads to mitochondrial swelling. Consequently, the outer membrane ruptures to release intermembrane proteins such as cytochrome c [43]. Anti-apoptotic BCL-2 family proteins (e.g. BCL-2, BCL-xL, BCL-W, A1, Mcl-1), contain BH domains 1-4 and are generally integrated within the outer mitochondrial membrane. These proteins function within the apoptotic pathway to directly bind and inhibit the pro-apoptotic BCL-2 family proteins. The pro-apoptotic BCL-2 family proteins are divided into two classes: the effector molecules (e.g. BAK and BAX), which contain BH1-3 domains and permeabilize the outer mitochondrial membrane by creating the proteolipid pore responsible for cytochrome c release; and the BH3-only proteins (e.g. BAD, BID, BIK, BIM, BMF, bNIP3, HRK, Noxa, PUMA) [44]. While pyrazole plus LPS treatment increased the expression of pro-apoptotic proteins (e.g. BAX, BID, BCL-xS) 2-2.5 fold in liver mitochondria, which may contribute to development of the MPT, CsA did not attenuate these increases. Thus CsA does not prevent the MPT by modulating levels of BCL-2 family members.

Peroxynitrite induces the MPT [45]. The elevated production of superoxide due to TNF-α plus CYP2E1 and the generation of nitric oxide due to induction of iNOS, promotes formation of peroxynitrite as evident from the increase in 3-NT protein adducts. We hypothesize that the initial generation of ROS/reactive nitrogen species from TNF-α, CYP2E1 and iNOS causes MPT, which then further elevates ROS production. CsA, by blocking MPT prevents this secondary enhanced production of ROS as reflected by CsA inhibition of 3-NT and HNE protein adduct formation.

Fig. 7 presents a scheme to summarize what we believe are main features in the pyrazole plus LPS liver injury model. LPS induces Kupffer cells to release TNF-α, while pyrazole induces hepatocyte CYP2E1 expression. TNF-α plus CYP2E1 promote an elevated oxidative stress while activates iNOS, p38 MAPK and JNK2. iNOS, p38 MAPK and JNK are also present in the mitochondria and it is possible that the pyrazole plus LPS-induced oxidative stress activates these enzymes in the mitochondrial compartment in addition to the cytosol. This remains to be determined. Increases in ROS production and MAPK activation results in an imbalance between anti- and pro-apoptotic BCL-2 family proteins, MPT, release of cytochrome c, and further production of ROS. The MPT, the loss of cytochrome c, and the mitochondrial oxidative stress results in hepatocyte necrosis. CsA prevents the MPT, blocks cytochrome c release from mitochondria, and lowers mitochondrial oxidative stress thereby protecting the hepatocyte from necrosis. These results support the concept that blocking MPT could be a strategy to treat alcohol liver injury.

Acknowledgements

This work was supported by USPHS grant AA-03312 from the National Institute on Alcohol Abuse and Alcoholism.

References

1. Rao RK, Seth A, Sheth P. Recent Advances in Alcoholic Liver Disease I. Role of intestinal permeability and endotoxemia in alcoholic liver disease. Am J Physiol Gastrointest Liver Physiol 2004;286:G881–884. [PubMed: 15132946]
2. Lu Y, Cederbaum AI. CYP2E1 and oxidative liver injury by alcohol. Free Radic Biol Med 2008;44:723–738. [PubMed: 18078827]
3. Ekstrom G, Ingelman-Sundberg M. Rat liver microsomal NADPH-supported oxidase activity and lipid peroxidation dependent on ethanol-inducible cytochrome P-450 (P-450IIE1). Biochem Pharmacol 1989;38:1313–1319. [PubMed: 2495801]
4. Lu Y, Wang X, Cederbaum AI. Lipopolysaccharide-induced liver injury in rats treated with the CYP2E1 inducer pyrazole. Am J Physiol Gastrointest Liver Physiol 2005;289:G308–319. [PubMed: 15845871]
5. Lu Y, Cederbaum AI. Enhancement by pyrazole of lipopolysaccharide-induced liver injury in mice: role of cytochrome P450 2E1 and 2A5. Hepatology 2006;44:263–274. [PubMed: 16799984]
6. Wu D, Cederbaum A. Cytochrome P4502E1 sensitizes to tumor necrosis factor alpha-induced liver injury through activation of mitogen-activated protein kinases in mice. Hepatology 2008;47:1005–1017. [PubMed: 18095305]
7. Nichols KD, Kirby GM. Microarray analysis of hepatic gene expression in pyrazole-mediated hepatotoxicity: identification of potential stimuli of Cyp2a5 induction. Biochem Pharmacol 2008;75:538–551. [PubMed: 17945193]
8. Juhaszova M, Wang S, Zorov DB, Bradley Nuss H, Gleichmann M, Mattson MP, Sollott SJ. The identity and regulation of the mitochondrial permeability transition pore: where the known meets the unknown. Ann N Y Acad Sci 2008;1123:197–212. [PubMed: 18375592]
9. Hunter DR, Haworth RA, Southard JH. Relationship between configuration, function, and permeability in calcium-treated mitochondria. J Biol Chem 1976;251:5069–5077. [PubMed: 134035]
10. Tsujimoto Y, Shimizu S. Role of the mitochondrial membrane permeability transition in cell death. Apoptosis 2007;12:835–840. [PubMed: 17136322]
11. Masubuchi Y, Suda C, Horie T. Involvement of mitochondrial permeability transition in acetaminophen-induced liver injury in mice. J Hepatol 2005;42:110–116. [PubMed: 15629515]
12. Haouzi D, Lekehal M, Tinel M, Vadrot N, Caussanel L, Letteron P, Moreau A, Feldmann G, Fau D, Pessayre D. Prolonged, but not acute, glutathione depletion promotes Fas-mediated mitochondrial permeability transition and apoptosis in mice. Hepatology 2001;33:1181–1188. [PubMed: 11343247]
13. Martin EJ, Forkert PG. Evidence that 1,1-dichloroethylene induces apoptotic cell death in murine liver. J Pharmacol Exp Ther 2004;310:33–42. [PubMed: 15028783]
14. Zhuge J, Cederbaum AI. Increased toxicity by transforming growth factor-beta 1 in liver cells overexpressing CYP2E1. Free Radic Biol Med 2006;41:1100–1112. [PubMed: 16962935]
15. Zhuge J, Cederbaum AI. Depletion of S-adenosyl-l-methionine with cycloleucine potentiates cytochrome P450 2E1 toxicity in primary rat hepatocytes. Arch Biochem Biophys 2007;466:177–185. [PubMed: 17640612]
16. Zhuge J, Cederbaum AI. Serum deprivation-induced HepG2 cell death is potentiated by CYP2E1. Free Radic Biol Med 2006;40:63–74. [PubMed: 16337880]
17. Rickmann M, Vaquero EC, Malagelada JR, Molero X. Tocotrienols induce apoptosis and autophagy in rat pancreatic stellate cells through the mitochondrial death pathway. Gastroenterology 2007;132:2518–2532. [PubMed: 17570223]
18. Kessova IG, Cederbaum AI. Mitochondrial alterations in livers of Sod1-/- mice fed alcohol. Free Radic Biol Med 2007;42:1470–1480. [PubMed: 17448893]
19. Poli G, Biasi F, Leonarduzzi G. 4-Hydroxynonenal-protein adducts: A reliable biomarker of lipid oxidation in liver diseases. Mol Aspects Med 2008;29:67–71. [PubMed: 18158180]
20. Tarpey MM, Wink DA, Grisham MB. Methods for detection of reactive metabolites of oxygen and nitrogen: in vitro and in vivo considerations. Am J Physiol Regul Integr Comp Physiol 2004;286:R431–444. [PubMed: 14761864]

21. Ischiropoulos H. Biological tyrosine nitration: a pathophysiological function of nitric oxide and reactive oxygen species. Arch Biochem Biophys 1998;356:1–11. [PubMed: 9681984]
22. Nieto N, Mari M, Cederbaum AI. Cytochrome P450 2E1 responsiveness in the promoter of glutamate-cysteine ligase catalytic subunit. Hepatology 2003;37:96–106. [PubMed: 12500194]
23. Dey A, Caro AA, Cederbaum AI. S-adenosyl methionine protects ob/ob mice from CYP2E1-mediated liver injury. Am J Physiol Gastrointest Liver Physiol 2007;293:G91–103. [PubMed: 17446309]
24. Wang Y, Singh R, Lefkowitch JH, Rigoli RM, Czaja MJ. Tumor necrosis factor-induced toxic liver injury results from JNK2-dependent activation of caspase-8 and the mitochondrial death pathway. J Biol Chem 2006;281:15258–15267. [PubMed: 16571730]
25. Gogvadze, V.; Orrenius, S.; Zhivotovsky, B. Current Protocols in Cell Biology. John Wiley & Sons, Inc.; 2003. Analysis of mitochondrial dysfunction during cell death; p. 18.15.11-18.15.27.
26. Youle RJ, Strasser A. The BCL-2 protein family: opposing activities that mediate cell death. Nat Rev Mol Cell Biol 2008;9:47–59. [PubMed: 18097445]
27. Thurman RG, Bradford BU, Iimuro Y, Knecht KT, Arteel GE, Yin M, Connor HD, Wall C, Raleigh JA, Frankenberg MV, Adachi Y, Forman DT, Brenner D, Kadiiska M, Mason RP. The role of gut-derived bacterial toxins and free radicals in alcohol-induced liver injury. J Gastroenterol Hepatol 1998;(13 Suppl):S39–50. [PubMed: 9792033]
28. McClain CJ, Song Z, Barve SS, Hill DB, Deaciuc I. Recent advances in alcoholic liver disease. IV. Dysregulated cytokine metabolism in alcoholic liver disease. Am J Physiol Gastrointest Liver Physiol 2004;287:G497–502. [PubMed: 15331349]
29. Arteel GE. Oxidants and antioxidants in alcohol-induced liver disease. Gastroenterology 2003;124:778–790. [PubMed: 12612915]
30. Nagy LE. Molecular aspects of alcohol metabolism: transcription factors involved in early ethanol-induced liver injury. Annu Rev Nutr 2004;24:55–78. [PubMed: 15189113]
31. Cederbaum AI. Introduction-serial review: alcohol, oxidative stress and cell injury. Free Radic Biol Med 2001;31:1524–1526. [PubMed: 11744324]
32. Albano E, Clot P, Morimoto M, Tomasi A, Ingelman-Sundberg M, French SW. Role of cytochrome P4502E1-dependent formation of hydroxyethyl free radical in the development of liver damage in rats intragastrically fed with ethanol. Hepatology 1996;23:155–163. [PubMed: 8550035]
33. Caro AA, Cederbaum AI. Oxidative stress, toxicology, and pharmacology of CYP2E1. Annu Rev Pharmacol Toxicol 2004;44:27–42. [PubMed: 14744237]
34. Liu H, Jones BE, Bradham C, Czaja MJ. Increased cytochrome P-450 2E1 expression sensitizes hepatocytes to c-Jun-mediated cell death from TNF-alpha. Am J Physiol Gastrointest Liver Physiol 2002;282:G257–266. [PubMed: 11804847]
35. Panov A, Dikalov S, Shalbuyeva N, Hemendinger R, Greenamyre JT, Rosenfeld J. Species- and tissue-specific relationships between mitochondrial permeability transition and generation of ROS in brain and liver mitochondria of rats and mice. Am J Physiol Cell Physiol 2007;292:C708–718. [PubMed: 17050617]
36. Hansson MJ, Mansson R, Morota S, Uchino H, Kallur T, Sumi T, Ishii N, Shimazu M, Keep MF, Jegorov A, Elmer E. Calcium-induced generation of reactive oxygen species in brain mitochondria is mediated by permeability transition. Free Radic Biol Med 2008;45:284–294. [PubMed: 18466779]
37. Zorov DB, Juhaszova M, Sollott SJ. Mitochondrial ROS-induced ROS release: an update and review. Biochim Biophys Acta 2006;1757:509–517. [PubMed: 16829228]
38. Garlid KD, Beavis AD. Evidence for the existence of an inner membrane anion channel in mitochondria. Biochim Biophys Acta 1986;853:187–204. [PubMed: 2441746]
39. Akar FG, Aon MA, Tomaselli GF, O'Rourke B. The mitochondrial origin of postischemic arrhythmias. J Clin Invest 2005;115:3527–3535. [PubMed: 16284648]
40. Zorov DB, Filburn CR, Klotz LO, Zweier JL, Sollott SJ. Reactive oxygen species (ROS)-induced ROS release: a new phenomenon accompanying induction of the mitochondrial permeability transition in cardiac myocytes. J Exp Med 2000;192:1001–1014. [PubMed: 11015441]
41. Malhi H, Gores GJ, Lemasters JJ. Apoptosis and necrosis in the liver: a tale of two deaths? Hepatology 2006;43:S31–44. [PubMed: 16447272]

42. Wei MC, Zong WX, Cheng EH, Lindsten T, Panoutsakopoulou V, Ross AJ, Roth KA, MacGregor GR, Thompson CB, Korsmeyer SJ. Proapoptotic BAX and BAK: a requisite gateway to mitochondrial dysfunction and death. Science 2001;292:727–730. [PubMed: 11326099]

43. Bradham CA, Qian T, Streetz K, Trautwein C, Brenner DA, Lemasters JJ. The mitochondrial permeability transition is required for tumor necrosis factor alpha-mediated apoptosis and cytochrome c release. Mol Cell Biol 1998;18:6353–6364. [PubMed: 9774651]

44. Chipuk JE, Green DR. How do BCL-2 proteins induce mitochondrial outer membrane permeabilization? Trends Cell Biol 2008;18:157–164. [PubMed: 18314333]

45. Radi R, Cassina A, Hodara R, Quijano C, Castro L. Peroxynitrite reactions and formation in mitochondria. Free Radic Biol Med 2002;33:1451–1464. [PubMed: 12446202]

Abbreviations

ALT
alanine aminotransferase

AST
aspartate aminotransferase

CsA
cyclosporine A

CYP2E1
cytochrome P450 2E1

GSH
glutathione

HNE
4-hydroxynonenal

iNOS
inducible nitric oxide synthase

JNK
c-Jun N-terminal kinase

LPS
lipopolysaccharide

MAPK
mitogen-activated protein kinase

MDA
malondialdehyde

MPT
mitochondrial permeability transition

3-NT
3-nitrotyrosine

ROS
reactive oxygen species

SOD2
manganese superoxide dismutase

TNF

tumor necrosis factor

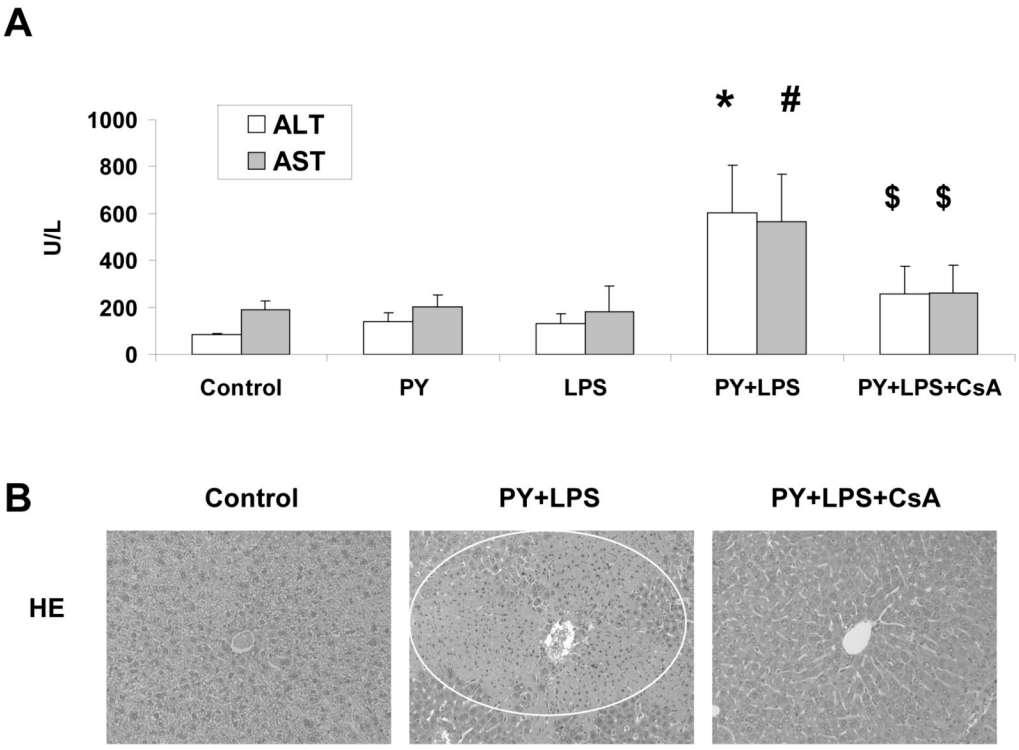

Fig. 1.

Cyclosporin A (CsA) protects mice from pyrazole (PY) plus lipopolysaccharide (LPS)-induced liver injury. (A) Serum alanine aminotransferase (ALT) and aspartate aminotransferase (AST) levels. Mice were treated with either PY, LPS, or PY plus LPS with or without CsA as described in Materials and Methods. Serums were assayed with Infinity ALT and AST liquid stable reagent. * $P<0.005$, # $P<0.05$, vs. control, PY or LPS groups, $ $P<0.05$, vs. PY+LPS group. (B) Morphology of liver. Liver sections were stained with hematoxylin and eosin (HE). Circle shows zonal necrosis. The images are representative of results from 6 control-, 9 PY+LPS-, and 9 PY+LPS+CsA-treated mice.

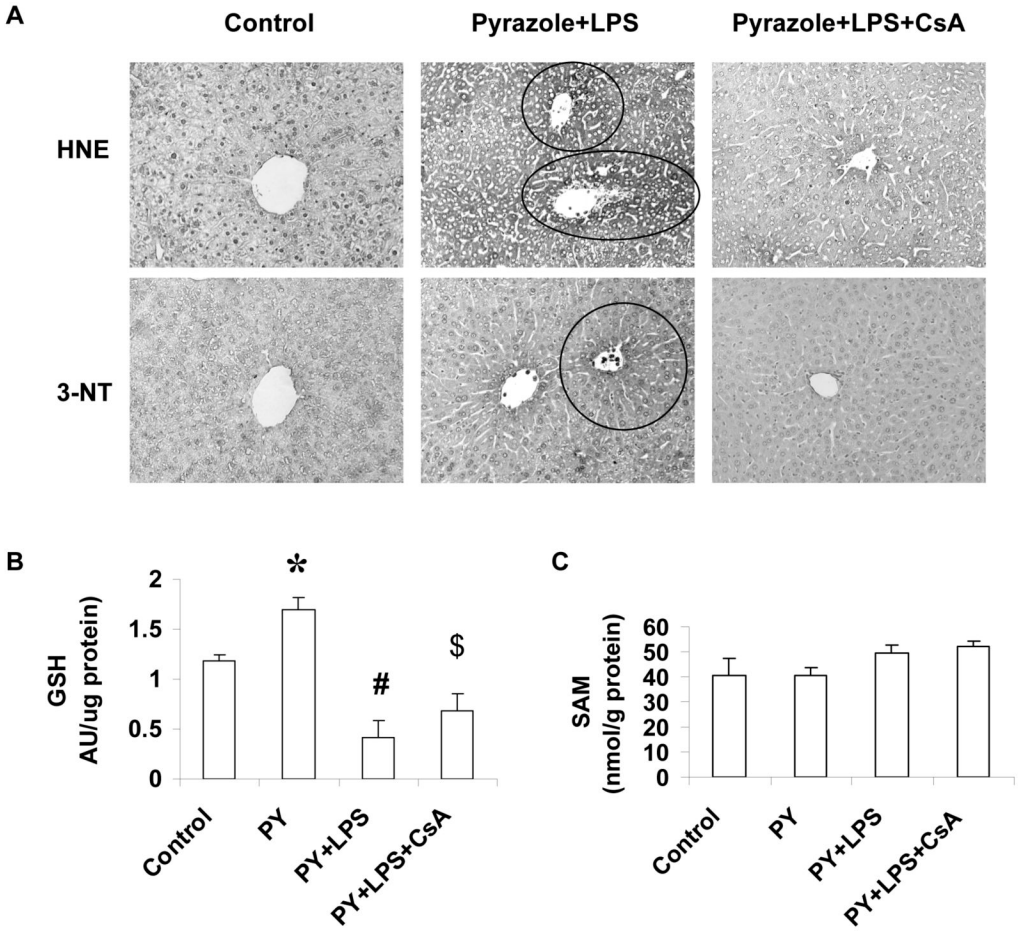

Fig. 2.

Cyclosporin A (CsA) protects mice from pyrazole (PY) plus lipopolysaccharide (LPS)-induced oxidative stress in liver. (A) Immunohistochemical staining of 4-hydroxynonenal (HNE) protein adducts and 3-nitrotyrosine (3-NT) protein adducts in liver tissue were carried out as described in Materials and Methods. Circles showed positive staining for HNE or 3-NT in liver sections. The images are representative of results from 6 control-, 9 PY+LPS-, and 9 PY+LPS +CsA-treated mice. (B) GSH levels in liver homogenate were assayed with the fluorometric substrate o-phthalaldehyde. *$P<0.05$, vs. control mice, #$P<0.005$ and $P<0.001$, vs. control and PY-treated mice, respectively, $ $P<0.05$, $P<0.001$, $P>0.05$, vs. control, PY-, PY plus LPS-treated mice, respectively. (C) Liver SAM levels were assayed by high performance liquid chromatography. No significant difference was found between the 4 groups.

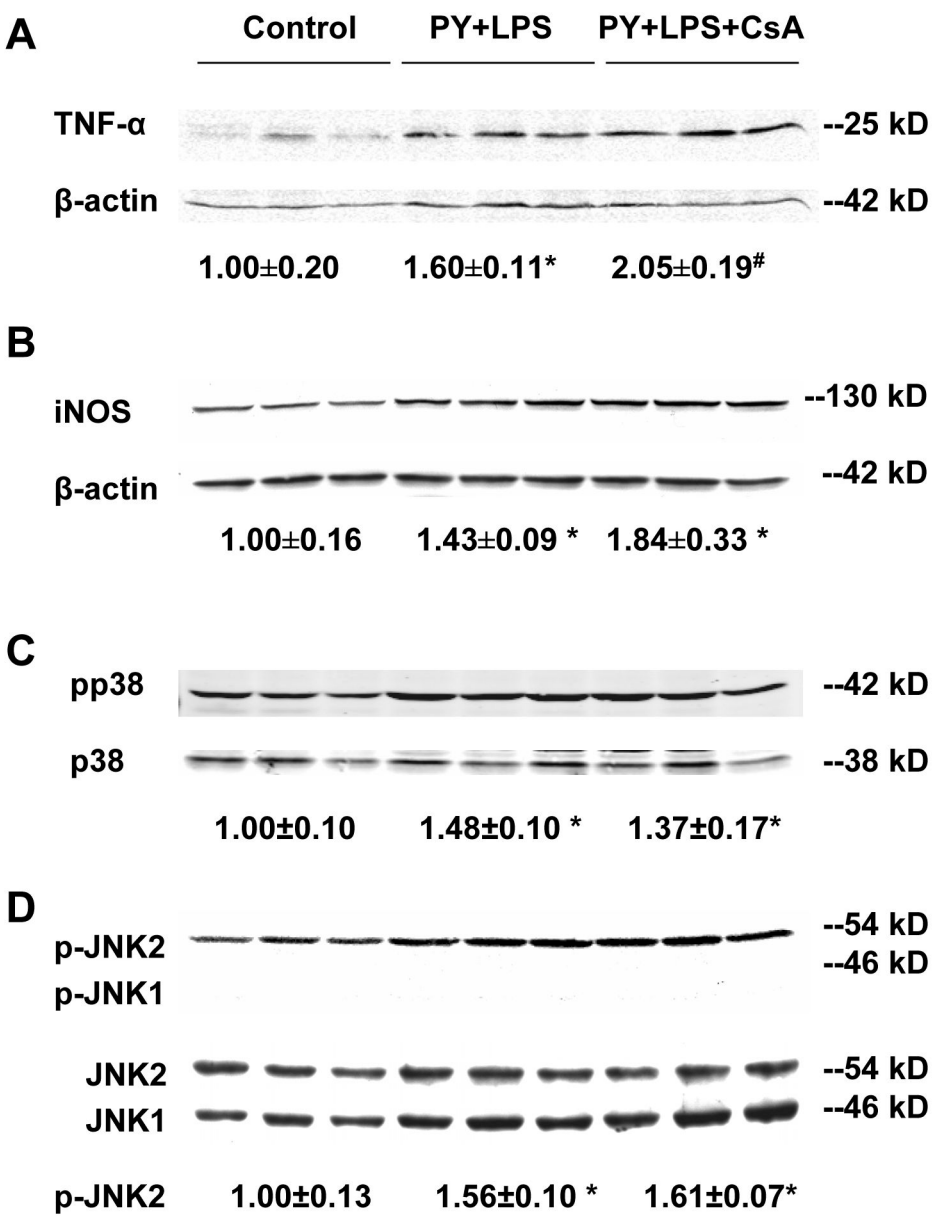

Fig. 3.

Levels of TNF-α, inducible nitric oxide synthase (iNOS) and activated p38 MAPK and JNK. (A) Western blot analysis of tumor necrosis factor (TNF)-α levels in liver homogenate subjected to 18% sodium dodecyl sulfate polyacrylamide gel electrophoresis (SDS-PAGE). Precursor of TNF-α (25 kD) is shown, *$P<0.05$, #$P<0.01$, vs. control mice. (B) Western blot analysis of iNOS levels in liver homogenate subjected to 8% SDS-PAGE. *$P<0.05$, vs. control mice. (C) Western blot analysis of phosphorylation of p38 MAPK. Liver homogenate subjected to 10% SDS-PAGE and immunoblotted with rabbit anti-p-p38 (Thy 180/Tyr 182) and p38 (H-147) antibodies as described in Materials and Methods. *$P<0.05$, vs. control mice. (D) Western blot analysis of c-Jun N-terminal kinase (JNK) with rabbit anti-JNK1 (C-17) and mouse anti-p-JNK (G7) antibodies. Anti-p-JNK (G7) antibody can react with phosphorylated JNK1, JNK2 and JNK3 at Thr-183 and Tyr-185. *$P<0.005$, vs. control mice. Numbers under

the blot refer to the mean ± SD of the ratio of TNF-α, iNOS to β-actin, pp38 to p38, p-JNK2 to JNK2 from 3 mice in each group.

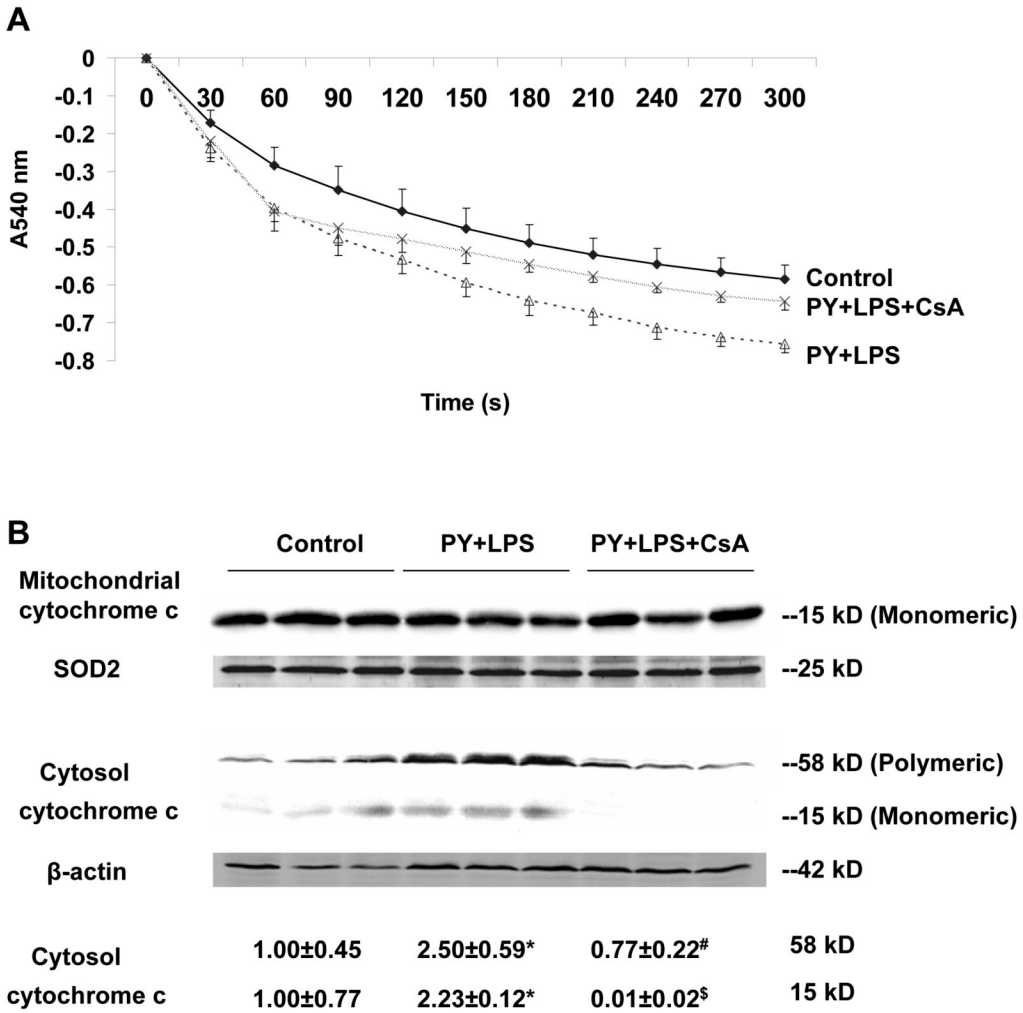

Fig. 4.

Mitochondrial swelling and release of mitochondrial cytochrome c. (A) Freshly prepared mitochondria, 0.5 mg/ml, were incubated in buffer containing 150 mM KCl, 10 mM Tris-MOPS, 5 mM glutamate, 2.5 mM malate, 1 mM KPi. Mitochondrial swelling was monitored by the decrease of absorbance at 540 nm (A540nm) after adding 100 μM of $CaCl_2$. (B) Western blot analysis of mitochondrial and cytosol cytochrome c. One hundred μg of liver mitochondrial or cytosolic protein was subjected to 18% sodium dodecyl sulfate polyacrylamide gel electrophoresis and immunoblotted with mouse anti-cytochrome c antibody and goat anti-SOD2 (G20) or mouse anti-β-actin antibody (C4) as mitochondrial or cytosolic loading control, respectively. The mitochondria cytochrome c migrates as a monomeric form (15 kD), and cytoplasmic cytochrome c exists as a monomeric form (15 kD) and a polymeric form (58-60 kD) by Western blot analysis (BD Pharmingen technical data sheet). Bands were quantified by the ImageJ image processing program. *P<0.05, vs. control mice. # P<0.01, $ P<0.005 vs. pyrazole plus LPS mice. Numbers under the blot refer to the mean ± SD of the ratio of the 58 kD and 15 kD of cytosol cytochrome c to β-actin from 3 mice in each group.

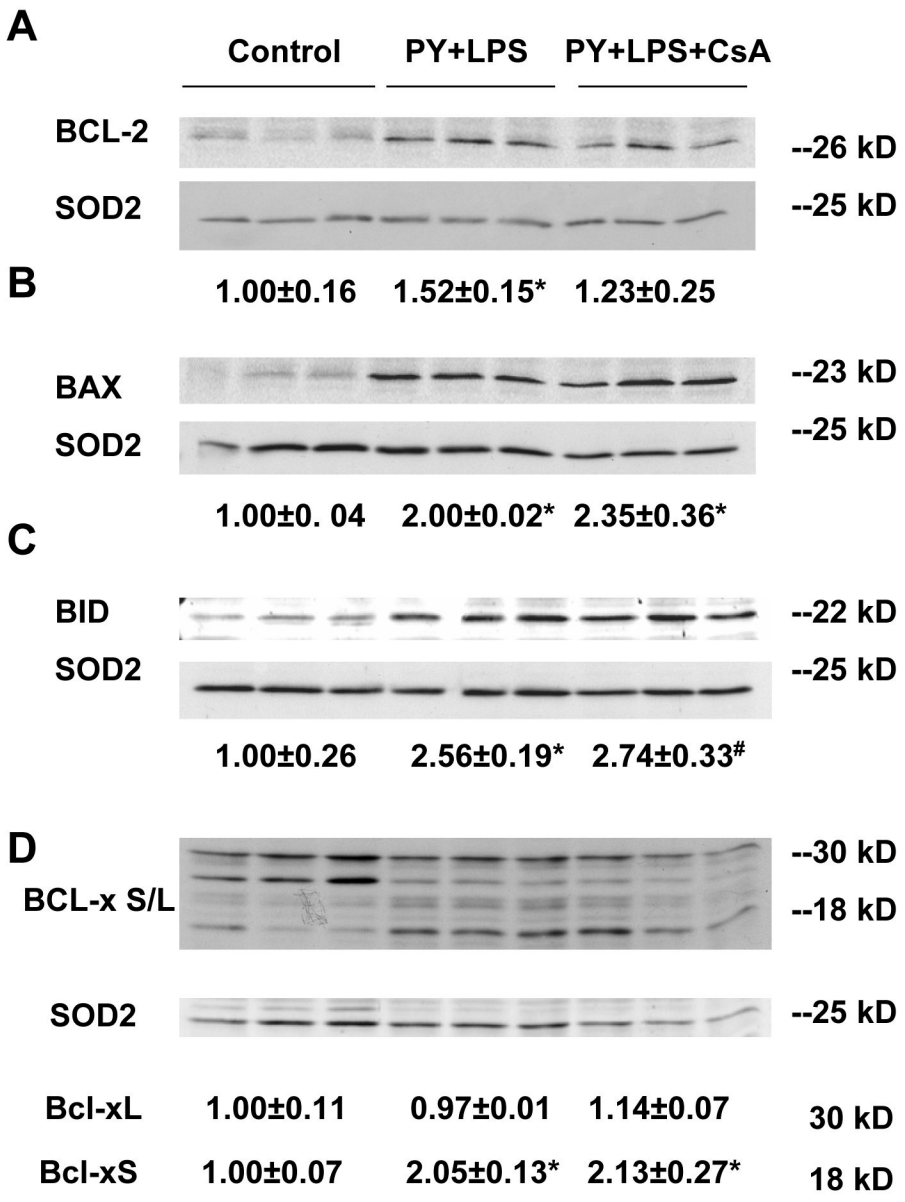

Fig. 5.

Western blot analysis of mitochondrial BCL-2 family protein levels. One hundred μg of liver mitochondrial protein was subjected to 18% sodium dodecyl sulfate polyacrylamide gel electrophoresis and immunoblotted with mouse anti-BCL-2 (C-2), rabbit anti-BAX (Ab-1), anti-BID (FL-195), anti-BCL-xS/L (L-19) antibodies and anti-SOD2 (G20) antibody as a mitochondrial loading control. Bands were quantified by the ImageJ image processing program. (A) BCL-2, **P*<0.05, vs. control. (B) BAX, **P*<0.005, vs. control. (C) BID, **P*<0.005, #*P*<0.001, vs. control. (D) BCL-Xs/L, **P*<0.005, vs. control. Numbers under the blot refer to the mean ± SD of the ratio of BCL-2, BAX, BID, BCL-xL and BCL-xS to SOD2 and are from 3 mice in each group.

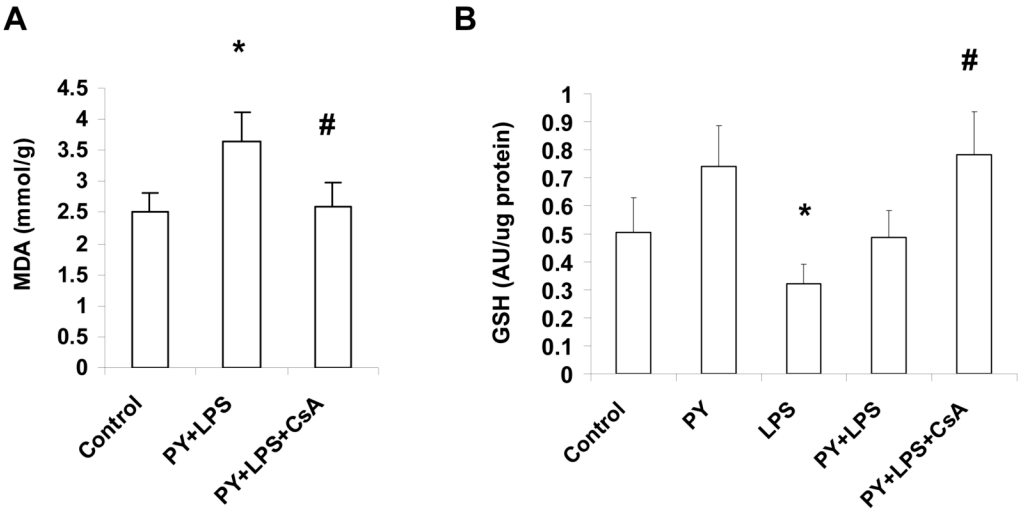

Fig. 6.

Malondialdehyde (MDA) and glutathione levels in mitochondria. (A) Mitochondrial lipid peroxidation. Measure of MDA levels with the thiobarbituric acid reactive substances assay. **P*<0.05, vs. control mice, #*P*<0.05, vs. pyrazole (PY) plus lipopolysaccharide (LPS)-treated mice. (B) Mitochondrial GSH levels. **P*<0.05, vs. PY alone-treated mice. #*P*<0.005, vs. LPS-treated mice, #*P*<0.05 vs. PY plus LPS-treated mice.

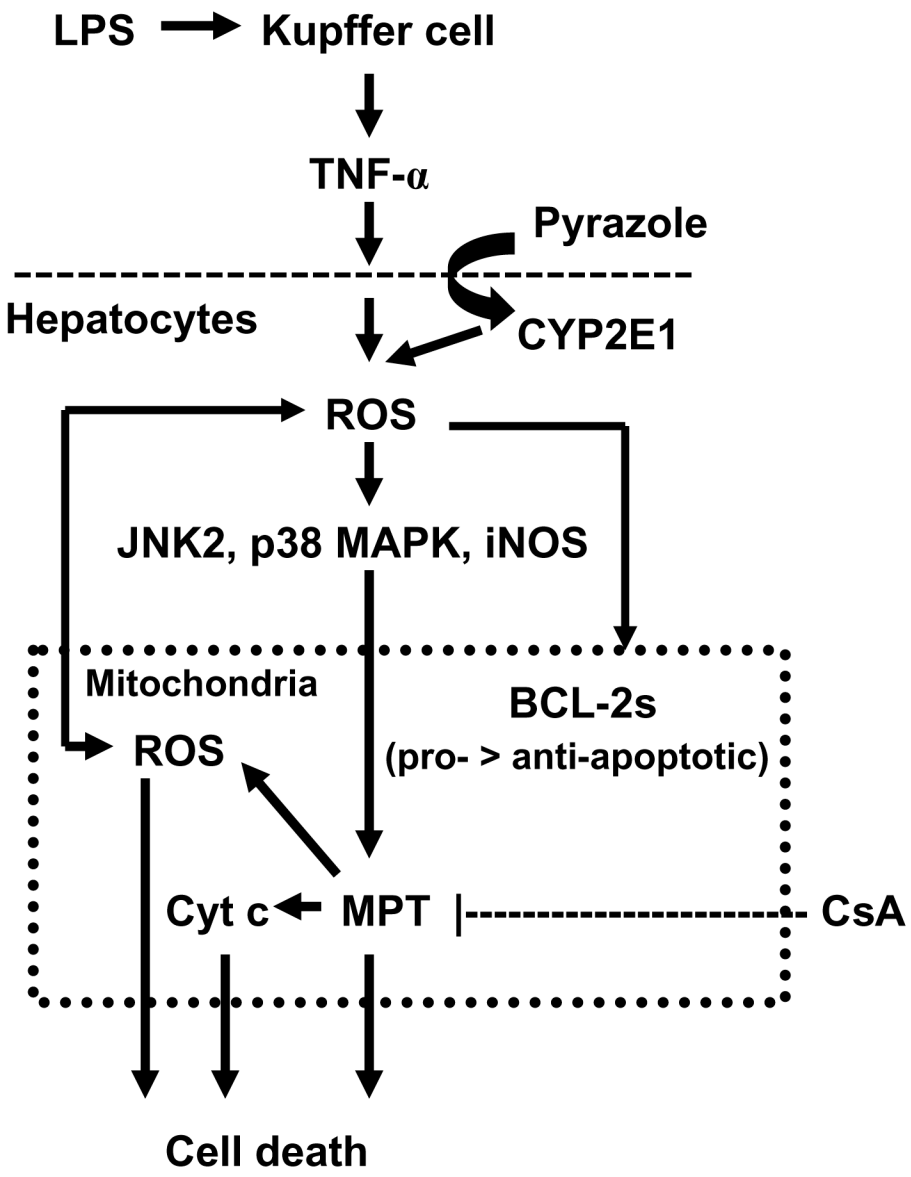

Fig. 7.

Scheme for the protection by cyclosporin A (CsA) against pyrazole plus lipopolysaccharide (LPS) liver injury. LPS induces Kupffer cells to release TNF-α, while pyrazole induces hepatocyte CYP2E1 expression. TNF-α plus CYP2E1 enhance production of ROS which can induce iNOS, and activate via phosphorylation p38 and JNK2 MAPK. Increases in ROS and reactive nitrogen species production, and activation of MAPK promotes an imbalance between anti-apoptic and pro-apoptotic BCL-2 family proteins, resulting in a mitochondrial permeability transition (MPT) and release of cytochrome c (Cyt c). This damage to the mitochondria increases production of ROS and causes hepatocyte necrosis. CsA prevents the MPT, blocks cytochrome c release from mitochondria, and lowers mitochondrial MDA, which protects the hepatocyte from the pyrazole plus LPS-induced necrosis.